JOURNAL OF GEOPHYSICAL RESEARCH, VOL. 106, NO. E10, PAGES 23,419–23,427, OCTOBER 25, 2001

Probing Mars' crustal magnetic field and ionosphere with the MGS Electron Reflectometer

D. L. Mitchell,[1] R. P. Lin,[1,2] C. Mazelle,[3] H. Rème,[3] P. A. Cloutier,[4]
J. E. P. Connerney,[5] M. H. Acuña,[5] and N. F. Ness[6]

Abstract. The Electron Reflectometer (ER) on board Mars Global Surveyor measures the energy and angular distributions of solar wind electrons and ionospheric photoelectrons. These data can be used in conjunction with magnetometer data to probe Mars' crustal magnetic field and to study Mars' ionosphere and solar wind interaction. During aerobraking, ionospheric measurements were obtained in the northern hemisphere at high solar zenith angles (SZAs, typically ~78°). The ionopause was crossed at altitudes ranging from 180 km to over 800 km, with a median of 380 km. The 400-km-altitude polar mapping orbit allows observations at SZAs from 25° to 155° in both the northern and southern hemispheres. The near-planet ionosphere and magnetotail structure of the night hemisphere is dominated by the presence of intense crustal magnetic fields, which can exceed 200 nT at the spacecraft altitude. Closed field lines anchored to highly elongated crustal sources form "magnetic cylinders," which exclude solar wind plasma traveling up the magnetotail. When the spacecraft passes through one of these structures, the ER count rate falls to the instrumental background, representing an electron flux drop of at least two orders of magnitude. A map of these flux dropouts in longitude and latitude closely resembles a map of the crustal magnetic sources. When the crustal magnetic cylinders rotate into sunlight, they fill with ionospheric plasma. Since many of these crustal fields are locally strong enough to stand off the solar wind to altitudes well above 400 km, the ionosphere can extend much higher than would otherwise be possible in the absence of crustal fields. Even weak crustal fields may locally bias the median ionopause altitude, which provides an indirect method of detecting crustal fields using ER observations.

1. Introduction

The Mars Global Surveyor (MGS) science payload includes two identical three-axis fluxgate magnetometers (MAG) and a symmetric hemispherical electrostatic analyzer (ER), which measures the energy and angular distributions of 10-eV to 20-keV electrons. The ER was designed to remotely probe crustal magnetic fields using the magnetic mirror effect, that is, the reflection of charged particles from regions of increased magnetic field strength [see *Acuña et al.*, 1992]. ER measurements provide the ratio of the field strength at the electron absorption altitude to that at the spacecraft. The absorption altitude at Mars varies with electron energy, ranging from ~200 km at 200 eV to ~120 km at 20 keV. Electron reflectometry thus can increase the sensitivity to crustal fields over that of an orbiting magnetometer alone, since the crustal field can be probed at altitudes well below that of the spacecraft.

After arriving at Mars on September 12, 1997, in a highly elliptical polar orbit, the MGS spacecraft aerobraked to achieve a ~400-km-altitude circular mapping orbit. The aerobraking orbits had periapsis at 105- to 175-km altitude, while apoapsis shrunk from an initial 17 R_M (1 R_M = 3393 km) to the mapping orbit on February 4, 1999. During aerobraking, ~20% of the Martian surface was mapped by the magnetometer at altitudes comparable to the electron absorption altitude [*Acuña et al.*, 1999]. The crustal field at Mars is much stronger than anticipated, and many crustal magnetic sources are easily measured directly by the magnetometer [*Connerney et al.*, 1999; *Ness et al.*, 1999], even at the 400-km mapping altitude [*Acuña et al.*, 2000]. The principal role of the ER to date has been to study the Mars plasma environment, which can be important for the proper interpretation of the magnetometer data, since magnetic fields arising from the solar wind interaction with Mars' ionosphere can be significant compared with crustal magnetic fields. The electron energy spectrum is diagnostic of the plasma environment and can be used in conjunction with magnetometer data to study the bow shock [*Vignes et al.*, 2000], magnetosheath [*Øieroset et al.*, 2000], ionosphere [*Cloutier et al.*, 1999; *Mitchell et al.*, 2000], and the process of ionization and loss of the neutral atmosphere [*Crider et al.*, 2000].

The MGS science phasing period (March 27 to September 13, 1998) provided 290 orbits for which the ER was operated continuously throughout the periapsis pass down to altitudes as low as 170 km. This unexpected data provided new and

[1]Space Sciences Laboratory, University of California, Berkeley, California.
[2]Also at Physics Department, University of California, Berkeley, California.
[3]Centre d'Etude Spatiale des Rayonnements, Toulouse, France.
[4]Department of Physics and Astronomy, Rice University, Houston, Texas.
[5]NASA Goddard Space Flight Center, Greenbelt, Maryland.
[6]Bartol Research Institute, University of Delaware, Newark, Delaware.

Paper number 2000JE001435.
0148-0227/01/2000JE001435$09.00

unique information about the Martian ionosphere [*Mitchell et al.*, 2000]. The ionosphere is separated from the solar wind by a plasma boundary, which is marked by a change in the electron energy spectrum. Above the boundary the electron population is dominated by the stagnating, mass-loaded solar wind as it flows past the planet. Below the boundary the electron population is dominated by atmospheric photoelectrons that are produced by solar ultraviolet and soft X-ray photons deep in the atmosphere and travel from the exobase (~180-km altitude) along magnetic field lines to the spacecraft, where they are measured. Although we do not measure thermal electrons (which have energies of ~0.3 eV at the >170-km altitudes sampled by the ER), comparison of our measurements with observations by Pioneer Venus Orbiter [*Spenner et al.*, 1980] suggests that this boundary is closely associated with the ionopause. Typically, an order-of-magnitude density contrast is observed across the boundary at energies near 1 keV, which implies effective magnetic separation between the ionospheric and solar wind plasmas. The fact that solar wind electrons have no access to magnetic field lines at altitudes well above the exobase implies that these fields are closed and thus likely to be of crustal origin. Thus the ER may be used to determine when the spacecraft is on crustal magnetic field lines.

As a result of the dynamic nature of the Mars–solar wind interaction, the ionopause boundary is highly structured and variable. On a single periapsis pass the spacecraft can make one or several ionopause crossings, suggesting a complex morphology with scale lengths of hundreds of kilometers and/or rapid motion (~1 km s^{-1}) of the boundary. During the science phasing period, nearly 90% of ionospheric observations were obtained at solar zenith angles >70° in the northern hemisphere, where crustal magnetic fields are relatively weak. The median ionopause altitude in this region is 380 km, although the ionopause altitude ranged from as low as 180 km to more than 800 km.

The nearly circular mapping orbit is fortuitously placed at an altitude of ~400 km, very close to the median ionopause altitude observed during the science phasing period. Thus the spacecraft makes numerous ionopause crossings as the boundary moves up and down in response to atmospheric and solar variability. The polar mapping orbit is fixed at a local time of 0200/1400, sampling solar zenith angles from ~30° to ~150°. There is uniform sampling in the northern and southern hemispheres, which allows us to study the effects of crustal magnetic fields on the ionosphere. Crustal fields can exceed 200 nT at the mapping altitude, which is much larger than typical fields resulting from the Mars–solar wind interaction (~20-50 nT).

2. Instrument Description

The Electron Reflectometer (ER) consists of a hemispherical imaging electrostatic analyzer followed by a microchannel plate (MCP) and a resistive imaging anode (Figure 1). The electrostatic analyzer is composed of two concentric hemispheres: the outer hemisphere is connected to spacecraft ground, and the inner hemisphere potential is adjusted to deflect electrons within a specified energy range onto the MCP. Each electron that hits the MCP produces a cloud of ~10^6 electrons, which in turn hits the resistive anode. The relative signal level at each end of the anode is measured by the pulse position analyzer (PPA) to determine the location on the anode where the electron cloud landed. Since the analyzer focuses (Figure 1, top view), this translates into the direction of the incident electron in the plane of the field of view (FOV). During a 2- to 48-s integration (depending on telemetry rate and energy) the ER samples electron fluxes in sixteen 22.5° × 14° sectors, which span the entire 360° × 14° field of view.

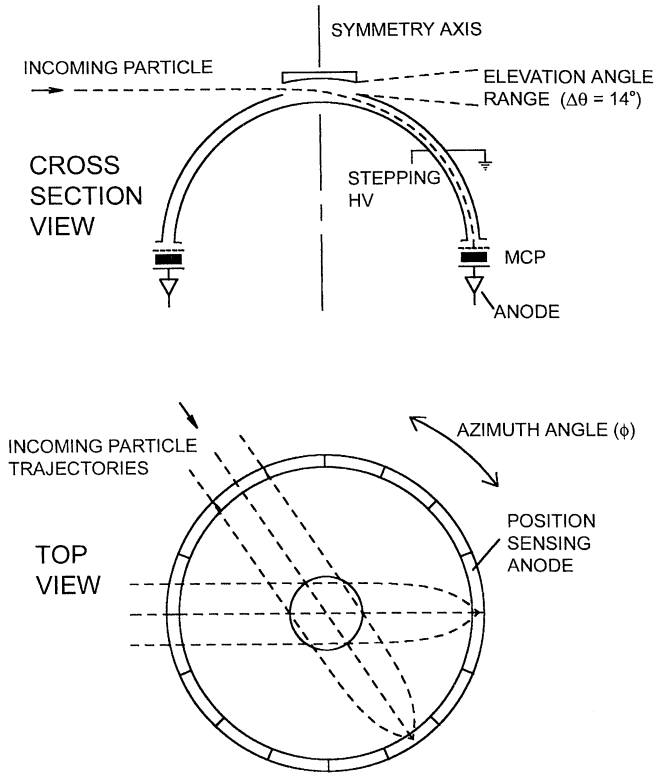

Figure 1. Schematic of the Electron Reflectometer showing the concentric hemispherical deflection plates, the microchannel plate (MCP) and the position-sensing resistive anode.

During each integration the ER measures electron fluxes in 30 logarithmically spaced energy channels ranging from 10 eV to 20 keV with an energy resolution of $\Delta E/E = 0.25$ (full width at half maximum (FWHM)). The instrument's energy scale is referenced to spacecraft ground. In sunlight, spacecraft ground typically floats a few volts positive relative to the plasma in which the spacecraft is immersed. Electrons are accelerated by the spacecraft potential before they can enter the ER aperture; thus all energies are shifted upward by a few eV. In addition to shifting the electron energy, the trajectories of low-energy electrons can be significantly bent by electric fields around the spacecraft. Thus the energy scale and imaging characteristics are relatively poor at the lowest energies (10–30 eV), becoming much more accurate at higher energies.

The FOV sweeps out the entire sky every half spin of the spacecraft (~50-60 minutes), which is much longer than most timescales of interest in Mars' plasma environment. Consequently, only ~12% of the electron angular distribution is sampled during an integration. With knowledge of the magnetic field vector measured on board, the FOV can be mapped into pitch angle α, which is the angle between an electron's instantaneous velocity and the magnetic field:

$$\cos(\alpha) = \cos(\phi - \phi_B)\cos(\theta_B)\,, \qquad (1)$$

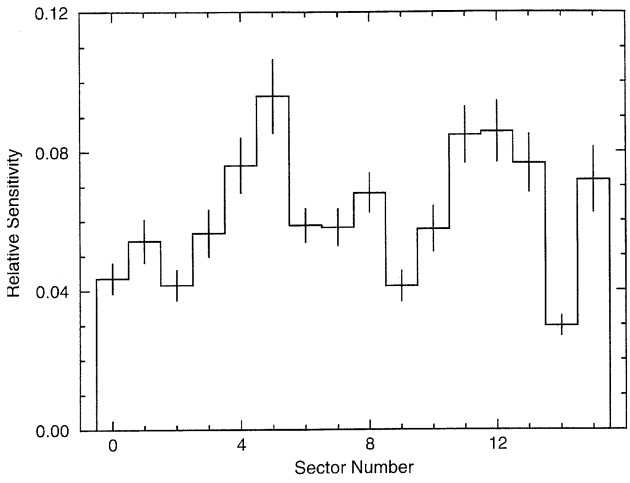

Figure 2. Relative sensitivity (with error bars) for the 16 angular sectors, each of which spans 22.5° in the field of view (FOV) plane. This is based on a calibration obtained shortly after deployment of the high-gain antenna.

where ϕ is the azimuth of the incident electron in the FOV plane and ϕ_B and θ_B are the azimuth and elevation of the magnetic field vector. During an integration the ER samples pitch angles from $|\theta_B|$ to $(180° - |\theta_B|)$. Because of the spacecraft's slow rotation, the field-aligned electron population (α = 0° or 180°) is sampled infrequently, whereas the 90° pitch angle population is always measured.

2.1 Geometric Factor and Dynamic Range

The geometric factor for the entire field of view is 0.02 cm^2 sr. The ER can use one of two entrance apertures, which cover the same FOV but differ in their transmission by a factor of 43.5. The smaller aperture (geometric factor of 4.6×10^{-4} cm^2 sr) is used to avoid saturation when measuring high fluxes at low energies. The larger aperture is used to maximize the sensitivity to low fluxes at high energies. The maximum count rate is limited by the time it takes the PPA to measure the azimuth of a single electron ($\tau = 4.8 \times 10^{-7}$ s), during which the instrument is insensitive to any other electrons. To correct for this deadtime, the measured count rate R is multiplied by the factor $(1 - R\tau)^{-1}$. To be conservative, we discard measurements where the correction factor is larger than 1.25, corresponding to a maximum corrected count rate of 5.2×10^5 counts per second (c s^{-1}). The background count rate (due to noise in the electronics and cosmic rays) is ~10 c s^{-1} at all energies. By using dual entrance apertures, we achieve a dynamic range of about six orders of magnitude.

The efficiency for detection varies around the FOV by a factor of three (Figure 2), because of gain variations across the MCP. This variation was calibrated after HGA deployment by taking advantage of the fact that the electron distribution at a given pitch angle is nearly independent of gyration phase around the magnetic field. Thus, if two sectors span the same pitch angle range, they should measure the same electron flux. When the magnetic field azimuth ϕ_B lines up with a sector boundary, there are eight independent pitch angle ranges that are observed simultaneously by two sectors each. As ϕ_B changes, different pairs of sectors line up, and eventually, all possible pairings occur. The flux ratios of all sector pairs are used to determine the relative sensitivity around the FOV. This procedure is overdetermined, allowing an estimate of the uncertainty, which is ~10%.

2.2 Sunlight and Spacecraft Photoelectron Effects

The ER is mounted on the instrument deck, with its symmetry axis (Figure 1) orthogonal to the spacecraft Z axis. The projection of the symmetry axis onto the spacecraft XY plane is 10° from the $-Y$ axis and 80° from the $+X$ axis. Parts of the spacecraft are within the instrument's FOV. During aerobraking the stowed high-gain antenna (HGA) blocked ~70°. After HGA deployment the only remaining blockage is caused by a corner of the spacecraft bus and the $-Y$ solar array gimbal and yoke assembly. Not only do these obstacles block solar wind and ionospheric electrons, but when they are illuminated by the Sun, they emit photoelectrons, which can enter the ER aperture, producing a time-varying signature that depends on the illumination pattern as the spacecraft rotates. The spacecraft photoelectron signal can be comparable to the signal from ambient electrons up to energies of ~80 eV. Electron measurements are free from this contamination for about half of the spacecraft spin.

For a duration of ~4 min every half spin of the spacecraft, sunlight can enter the aperture and scatter inside the instrument, creating secondary electrons. A tiny fraction of these photons and secondary electrons scatter down to the anode and generate a pulse of spurious counts. This sunlight pulse appears at all energies but is most noticeable from 10 to 80 eV and above 1 keV.

3. Summary of Aerobraking Results

Throughout most of aerobraking, periapsis was targeted for the 3.5-nbar pressure level (~120-km altitude), which exceeds the maximum pressure that the ER can be safely operated. (At pressures above ~1 nbar, there is risk of electrical dis-

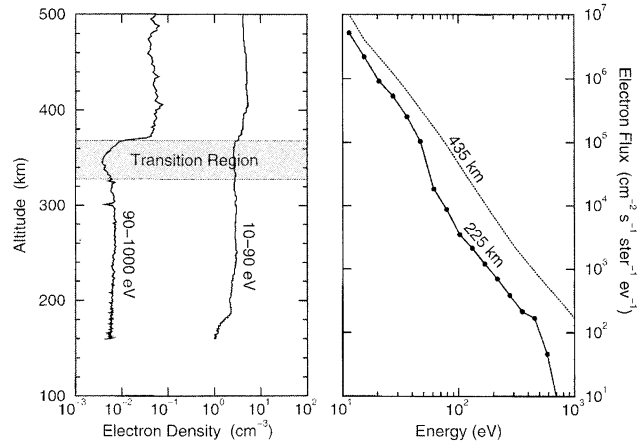

Figure 3. (left) Electron density in two energy ranges versus altitude measured outbound from periapsis number 215 on April 2, 1998. (right) Electron energy spectra at two altitudes measured on the same periapsis pass. Solid circles on the low-altitude spectrum indicate the individual energy channels. Error bars that account for counting statistics and digitization noise are smaller than the symbol size; however, we assume that the magnetic field and plasma are stationary during the 12-s accumulation time for each spectrum.

charge inside the instrument.) Because of Mars' atmospheric variability and uncertainty in predicting the time of periapsis, the ER high voltage was disabled below altitudes of ~350 km. However, the aerobraking phase included 290 "science phasing" orbits with periapsis at ~170 km (0.02 nbar), where there was ample safety margin for operating the ER. These orbits provided an opportunity to observe 10-eV to 20-keV electrons in Mars' ionosphere.

During the science phasing period the periapsis altitude was low enough that the spacecraft entered the ionosphere on every orbit. On each periapsis pass the ER consistently observed a transition region with a vertical thickness of tens of kilometers, where electron fluxes at energies greater than ~100 eV change by about an order of magnitude (Figure 3). This is accompanied by a change in the shape of the electron energy spectrum. Above the boundary, electron energy spectra are consistent with solar wind electrons that have been shocked and then modified by impact with exospheric neutrals [*Crider et al.*, 2000]. Below the boundary, electron energy spectra exhibit a broad feature from 20 to 50 eV, which likely results from a blend of unresolved photoionization peaks that have been predicted by published models of ionospheric photoelectrons at Mars [*Fox and Dalgarno*, 1979; *Mantas and Hanson*, 1979]. A second feature at ~500 eV results from oxygen Auger electrons (*Mitchell et al.*, 2000).

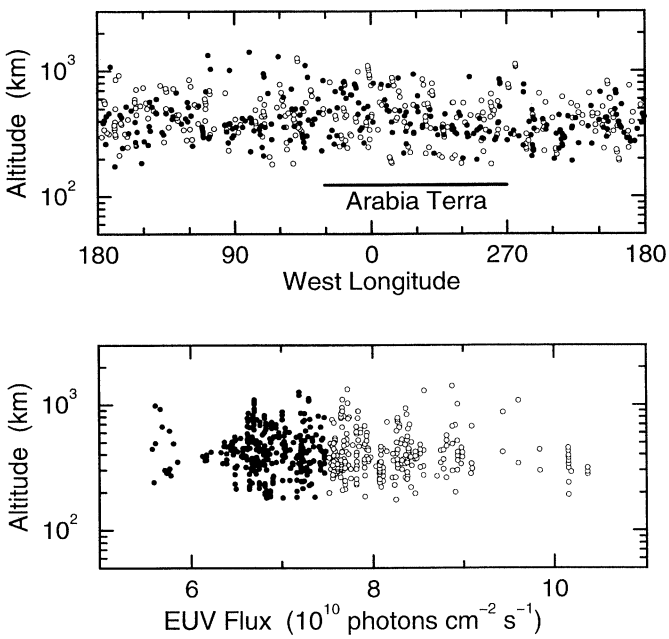

Figure 4. (top) Ionopause altitudes for periapsis passes from March 27 to September 13, 1988, are plotted as a function of the planetocentric longitude of the spacecraft at the time of the ionopause crossing. All ionopause crossings occurred in the northern hemisphere. The longitude range of Arabia Terra, the most strongly magnetized region in the northern hemisphere, is shown by the horizontal bar. (bottom) The same data plotted as a function of the total solar flux between wavelengths of 2 nm and 100 nm, as derived from the *F*10.7 radio flux measured at Earth [*Tobiska and Eparvier*, 1997] and time shifted on a point-by-point basis (assuming a 26-day solar rotation) to account for the different orbital positions of Earth and Mars. Solid (open) symbols in both plots indicate data obtained when the EUV flux was less (more) than 7.5×10^{10} photons cm^{-2} s^{-1}.

Table 1. Ionopause Location

Orbit	SZA[a]	Latitude	Mean Altitude, km	Median Altitude, km
203–266	43°–84°	13°–68°	380 ± 160	330
329–553	65°–90°	1°–86°	440 ± 180	390
all			430 ± 180	380

[a] Solar zenith angle.

A similar transition region, dubbed the "mantle," was observed at Venus by the Pioneer Venus Orbiter [*Spenner et al.*, 1980]. The lower boundary of the Venus mantle is coincident with the ionopause, as inferred by measurements of ions and thermal electrons. Although we do not measure thermal electrons, the similarity between our transition region and the Venus mantle suggests that the transition region is associated with Mars' ionopause. This interpretation is supported by the large electron flux contrast that is typically observed across the transition region, implying effective magnetic separation between a region dominated by photoelectrons and one dominated by solar wind electrons. This

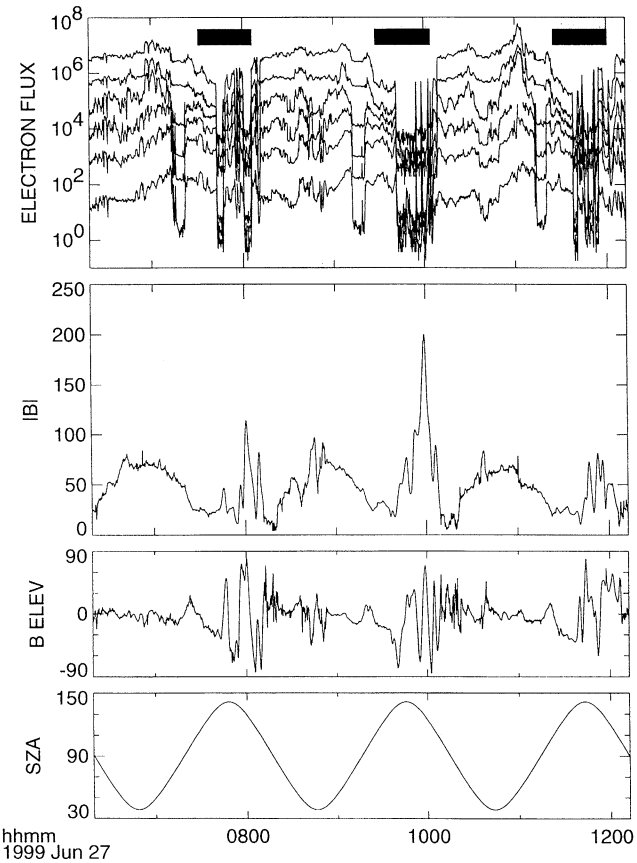

Figure 5. The top panel shows the omnidirectional electron flux (cm^{-2} s^{-1} sr^{-1} eV^{-1}) in six energy channels (from top to bottom: 10, 30, 60, 130, 280, and 750 eV). The solid bar indicates when the spacecraft is in Mars' shadow. The next two panels show the magnetic field amplitude (nT) and "magnetic elevation," which is the angle that the magnetic field vector makes with respect to the surface tangent plane (0° = horizontal field, +90° = radial outward, −90° = radial inward). The bottom panel shows the solar zenith angle. The polar orbit is locked at a local time of 0200/0400.

implies that magnetic field lines populated by only photoelectrons are closed to the solar wind and are therefore likely to be of crustal origin.

Ionopause altitudes for 290 science phasing orbits are shown in Figure 4. Occasionally, the spacecraft passed through the ionopause multiple times on a single periapsis pass, indicating a complex morphology with scale lengths of hundreds of kilometers and/or rapid motion (~1 km s^{-1}) of the boundary. Similar observations at Venus have been interpreted as surface waves [*Brace et al.*, 1980], possibly generated by the Kelvin-Helmholtz instability [*Elphic and Ershkovich*, 1984]. Since the observed multiple crossings occurred at high solar zenith angles (SZA > 60°), they could also result from detached ionospheric "clouds," which are also thought to occur at Venus [*Brace et al.*, 1987]. Multiple ionopause crossings are included in Figure 4, although some of these might result from detached clouds.

Since periapsis occurred within 30° of the north pole and there was negligible change in the orbital eccentricity throughout the 5-month measurement period, low solar zenith angles are always encountered at high altitudes. This sampling bias precludes us from investigating the solar zenith angle dependence of the ionopause altitude; however, the longitude sampling is unbiased.

The median ionopause altitude is 380 km, which is comparable to that observed at Venus at similar solar zenith angles

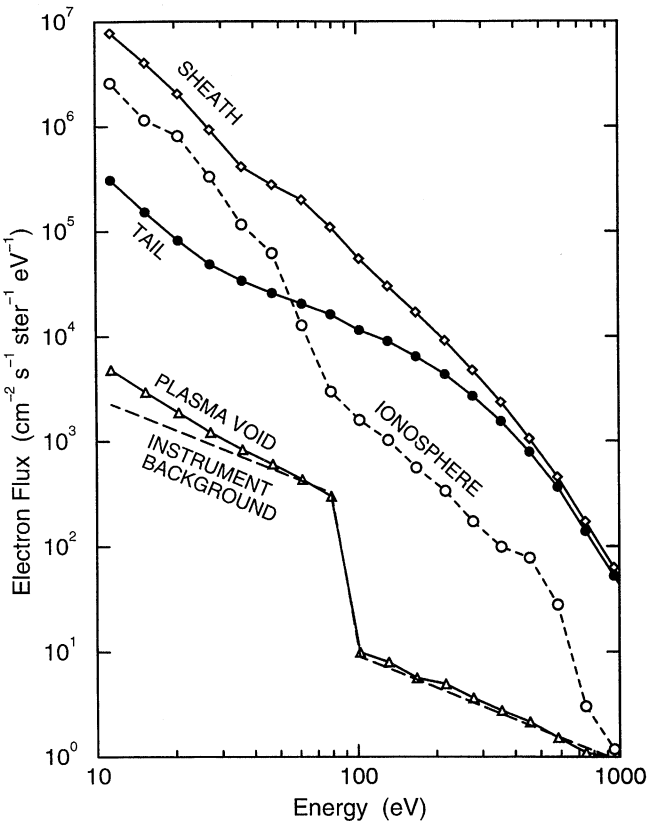

Figure 7. Electron energy spectra that define the different plasma regions identified in Figure 6.

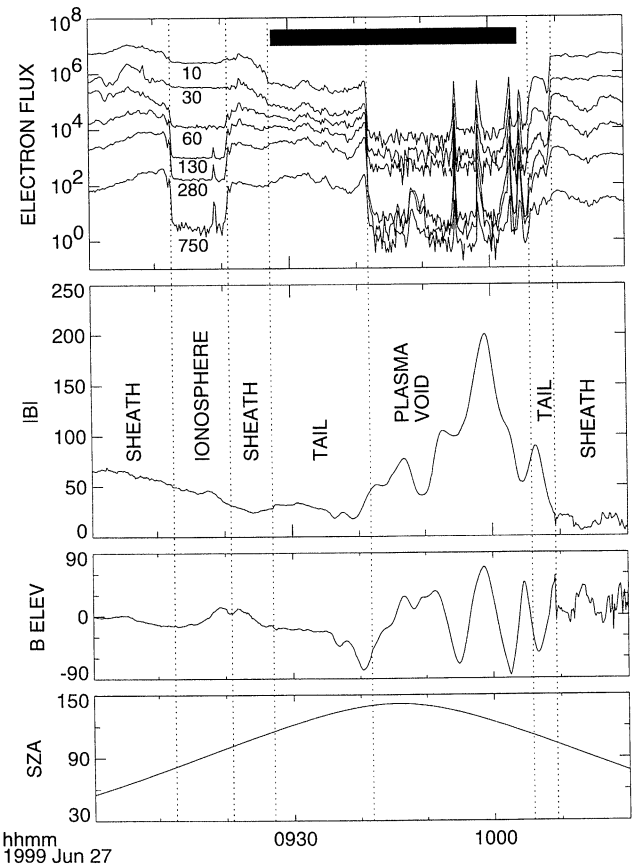

Figure 6. An expanded view of one of the plasma voids shown in Figure 5, divided into seven distinct plasma regions (vertical dashed lines) on the basis of electron energy spectra (see Figure 7). Electron flux spikes within the plasma void tend to occur when the magnetic field has a large radial component.

during solar moderate conditions [*Knudsen*, 1988]. The large variability in the ionopause altitude at Mars might result from changes in the solar wind dynamic pressure, the EUV flux, and occasional pressure support from crustal magnetic fields, which rotate with the planet. Although we lack the necessary instrumentation to estimate the solar wind dynamic pressure, we can search for evidence of ionopause control by solar EUV and/or crustal magnetic fields.

Ionopause altitudes are sorted by the planetocentric longitude of the spacecraft at the time of the crossing (Figure 4, top). All ionopause crossings occurred in the northern hemisphere (Table 1), where the strongest crustal magnetic fields are located over Arabia Terra, at latitudes south of ~45°N and between longitudes of about 30°W and 90°E (Plate 1). Because of the shape of the science phasing orbits, the spacecraft passed over these crustal fields at altitudes > 400 km. If the ionopause is systematically higher or if localized crustal "magnetospheres" extend to altitudes above 400 km over Arabia Terra, then one might expect an increase in the number of high-altitude (and possibly multiple) ionopause crossings between longitudes of 30°W and 90°E in Figure 4. The limited data obtained during the science phasing period provide no clear evidence for this effect. The much larger data set obtained in the 400-km-altitude mapping orbit will provide a far more sensitive probe of such effects over Arabia Terra and over the stronger crustal fields in the southern hemisphere (see section 5).

Ionopause altitudes are also sorted by an estimate of the solar EUV flux at the time of the crossing (Figure 4, bottom). The total solar flux between wavelengths of 2 and 100 nm is derived using the $F10.7$ radio flux measured at Earth as a

proxy [*Tobiska and Eparvier*, 1997], then scaled by the inverse square of the distance to the Sun and time shifted on a point-by-point basis to account for the time it takes a solar active region to rotate from facing Earth to facing Mars (assuming a 26-day solar rotation). Although the ionospheric photoelectron flux at Mars responds to changes in solar activity [*Mitchell et al.*, 2000], there is no evidence for a correlation of ionopause altitude with EUV flux, at least over the observed range of solar activity (near the minimum of the solar cycle). Large changes in the ionopause altitude from orbit to orbit and multiple ionopause crossings on some orbits raise the possibility that boundary variability arising from the solar wind interaction is large enough to obscure any systematic correlations with EUV flux and crustal magnetic fields, at least with the limited data set obtained during the science phasing period.

4. Observations From the Mapping Orbit

The 400-km-altitude, 0200-LT/1400-LT polar mapping orbit is close to the median ionopause altitude observed at high solar zenith angles during aerobraking. Because of the large ionopause variability, the spacecraft should make numerous ionopause crossings as the boundary moves up and down. A time series of electron and magnetic field measurements during three consecutive mapping orbits is shown in Figure 5. The magnetic field amplitude profile over the sunlit hemisphere approximately repeats from orbit to orbit, with local maxima near low solar zenith angles. This pattern would be expected for fields arising from the solar wind interaction with the ionosphere. The 75-nT field strength at solar zenith angles of 38° suggests a relatively high solar wind dynamic pressure. (Peak magnetic field strengths in the magnetosheath are more typically 20–50 nT, corresponding to magnetic pressures of $0.2–1.0 \times 10^{-8}$ dyn cm^{-2}, which are comparable to the expected range of solar wind dynamic pressures at Mars [*Zhang et al.*, 1990].) Fields as strong as 200 nT on the night hemisphere originate from crustal magnetic sources. These crustal fields are also distinguished by their relatively large and rapid variations in the magnetic field elevation (Figure 5). Large and sudden variations in the electron flux with corresponding changes in the electron energy spectrum indicate that the spacecraft is passing through several distinct plasma environments.

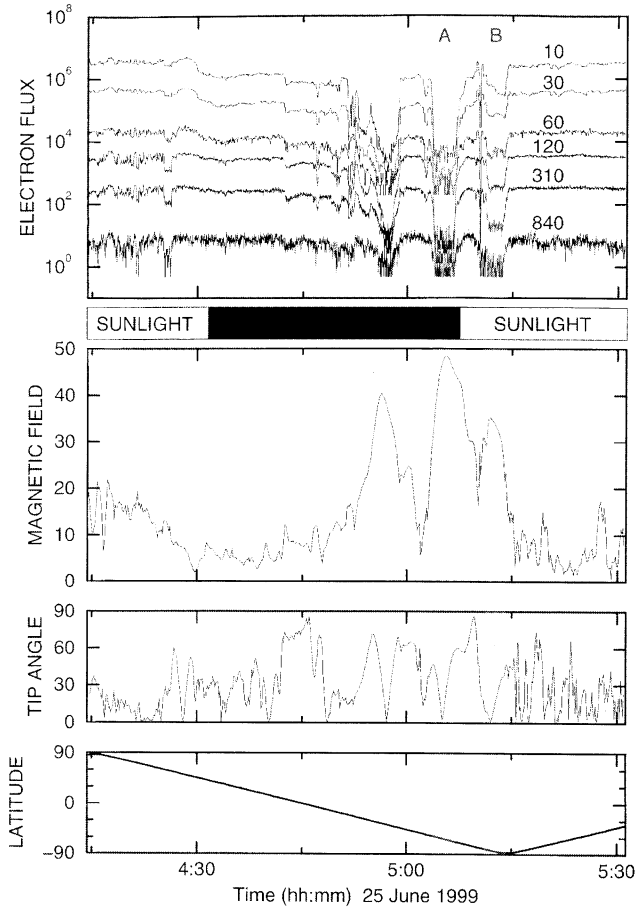

Figure 9. Time series of electron and magnetic field measurements obtained when two adjacent regions of closed crustal field lines straddled the terminator. The top panel shows the omnidirectional electron flux (cm^{-2} s^{-1} sr^{-1} eV^{-1}) in six energy channels (from top to bottom: 10, 30, 60, 120, 310, and 840 eV). The solid bar indicates when the spacecraft is in sunlight or darkness. The next two panels show the magnetic field amplitude (nT) and "tip angle," which is the acute angle that the magnetic field vector makes with respect to the surface tangent plane (0° = horizontal field, 90° = radial). The bottom panel shows the spacecraft latitude. Shaded region A is a plasma void, while shaded region B contains ionospheric plasma. Both shaded regions are bounded by solar wind plasma.

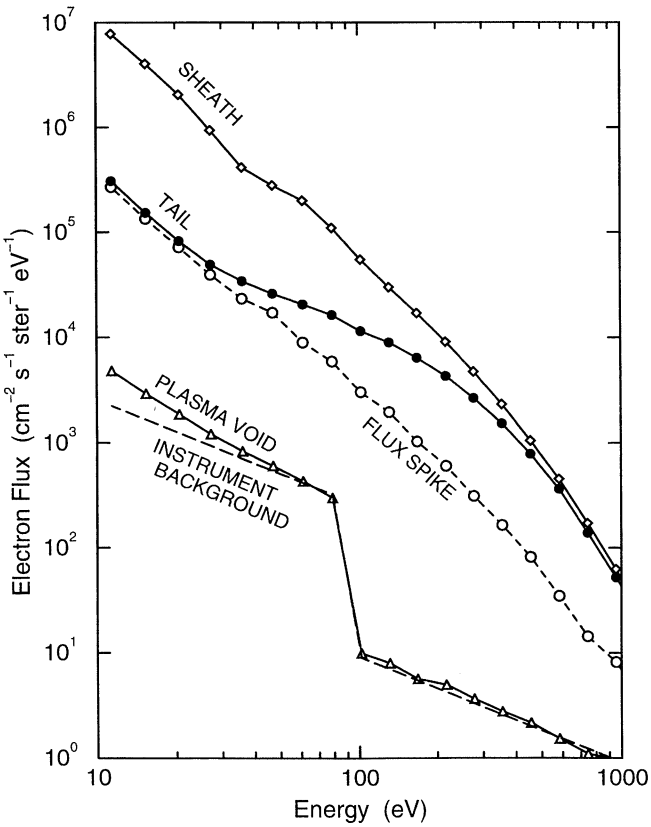

Figure 8. The electron energy spectrum within one of the flux spikes shown in Figure 6 is similar to the magnetosheath spectrum, except that the flux level is much lower.

An expanded view of one of these orbits shown in Figure 6. Different plasma environments, as inferred from electron energy spectra (Figure 7), are separated by vertical dashed lines. The magnetosheath spectrum is consistent with solar wind electrons that have been shocked and then modified by electron impact ionization of exospheric neutrals [*Crider et al.*, 2000]. The magnetotail and magnetosheath spectra coincide at energies above 400 eV, but lower-energy electrons are strongly attenuated in the magnetotail, since the spacecraft is in the solar wind wake immediately behind the planet. Low-energy electrons that might travel along the magnetic field into the wake are excluded by an electrostatic potential that forms at the wake boundary to prevent the buildup of charge. The ionospheric spectra are typical of photoelectron spectra observed during the science phasing period [*Mitchell et al.*, 2000].

When the spacecraft is in Mars' optical shadow, there are times when the instrumental count rate falls abruptly by up to three orders of magnitude to near background levels at all energies. We refer to these regions as "plasma voids," although there is a small but significant electron flux in the lowest-energy channels (Figure 7). These plasma voids occur in association with strong crustal magnetic fields in Figures 5 and 6, revealing that solar wind and ionospheric plasma are excluded from some crustal magnetic field lines. Plate 1 maps the locations of orbit segments when the spacecraft was within a plasma void over the course of 48 orbits from June 24 to 30, 1999. These orbit segments are overlain on a map of the radial component of the crustal magnetic field [*Acuña et al.*, 1999]. Plasma voids are closely associated with crustal magnetic sources. We infer that inside a plasma void, the spacecraft is on closed crustal magnetic field lines, which are effectively cut off from solar wind plasma traveling up the magnetotail and from ionospheric plasma from the sunlit hemisphere.

Often, a series of plasma voids are separated by electron "flux spikes," where the energy spectrum briefly returns to a magnetosheath distribution but with a reduced flux level at all energy channels (Figure 8). Flux spikes can occur over time intervals as short as 8 s, during which the spacecraft moves ~27 km along its orbit. Furthermore, the flux spikes tend to occur where the radial component of the crustal field is near a local maximum (inward or outward; see Figure 6). The presence of electrons with a magnetosheath-like energy spectrum indicates that these crustal magnetic field lines were at one time connected to the interplanetary magnetic field. Over the most strongly magnetized region (120°–210°W), narrow gaps between the plasma void orbit segments follow quasi-linear trends that are aligned with the linear magnetic sources (Plate 1). These gaps define the locus of electron flux spikes. This situation is similar to the cusp regions of the Earth's magnetosphere, except that the Martian cusps are quasi-linear over distances in excess of 2000 km. East-west trending arcades of closed field lines separated in latitude by quasi-linear cusps of alternating polarity suggest a series of magnetic "cylinders."

When these magnetic cylinders rotate into sunlight, they should become populated with photoelectrons produced from the enclosed neutral atmosphere. Figure 9 shows a time series of MAG/ER data in which two magnetic cylinders straddle the terminator. For the cylinder in darkness, the electron energy spectrum is indistinguishable from instrument background (Figure 10). However, electron energy spectra within the sunlit cylinder exhibit the characteristic features of atmospheric photoelectrons. Since the strongest crustal fields are capable of standing off the solar wind at altitudes well above the 400-km spacecraft orbit, the enclosed ionospheric plasma should remain trapped and shielded from the solar wind.

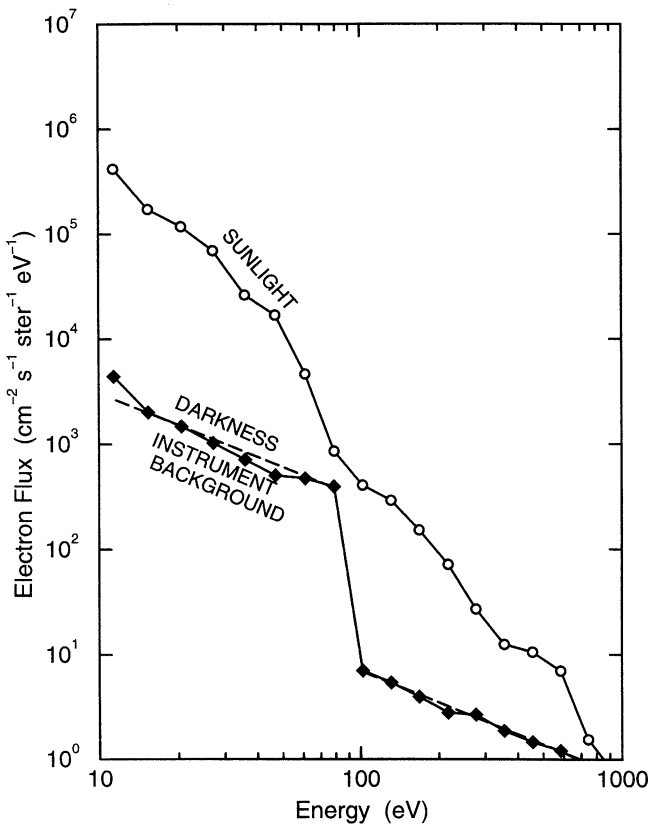

Figure 10. Electron energy spectra obtained in shaded regions A (darkness) and B (sunlight) of Figure 9.

5. Summary and Future Work

Because Mars lacks a global magnetic field, the solar wind interacts directly with the atmosphere/ionosphere over much of the planet. As a result of this interaction, a plasma boundary is formed at a median altitude of 380 km (SZA ~ 78°) that separates ionospheric and solar wind plasmas. This boundary is readily detected by the ER because the energy spectra of ionospheric and solar wind electrons are distinct. By comparison with more extensive observations at Venus, we conclude that the plasma boundary observed at Mars is likely associated with the ionopause. Typically, an order-of-magnitude density contrast is observed across the ionopause at energies near 1 keV, implying effective magnetic separation of the ionospheric and solar wind plasmas.

As a result of the dynamic nature of the Mars–solar wind interaction, the ionopause boundary is highly structured and variable. On a single periapsis pass the spacecraft can make one or several ionopause crossings, suggesting a complex morphology with scale lengths of hundreds of kilometers and/or rapid motion (~1 km s^{-1}) of the boundary. During the science phasing period, photoelectron fluxes were observed to correlate with solar EUV; however, there was no clear dependence of the ionopause altitude on solar EUV or on the

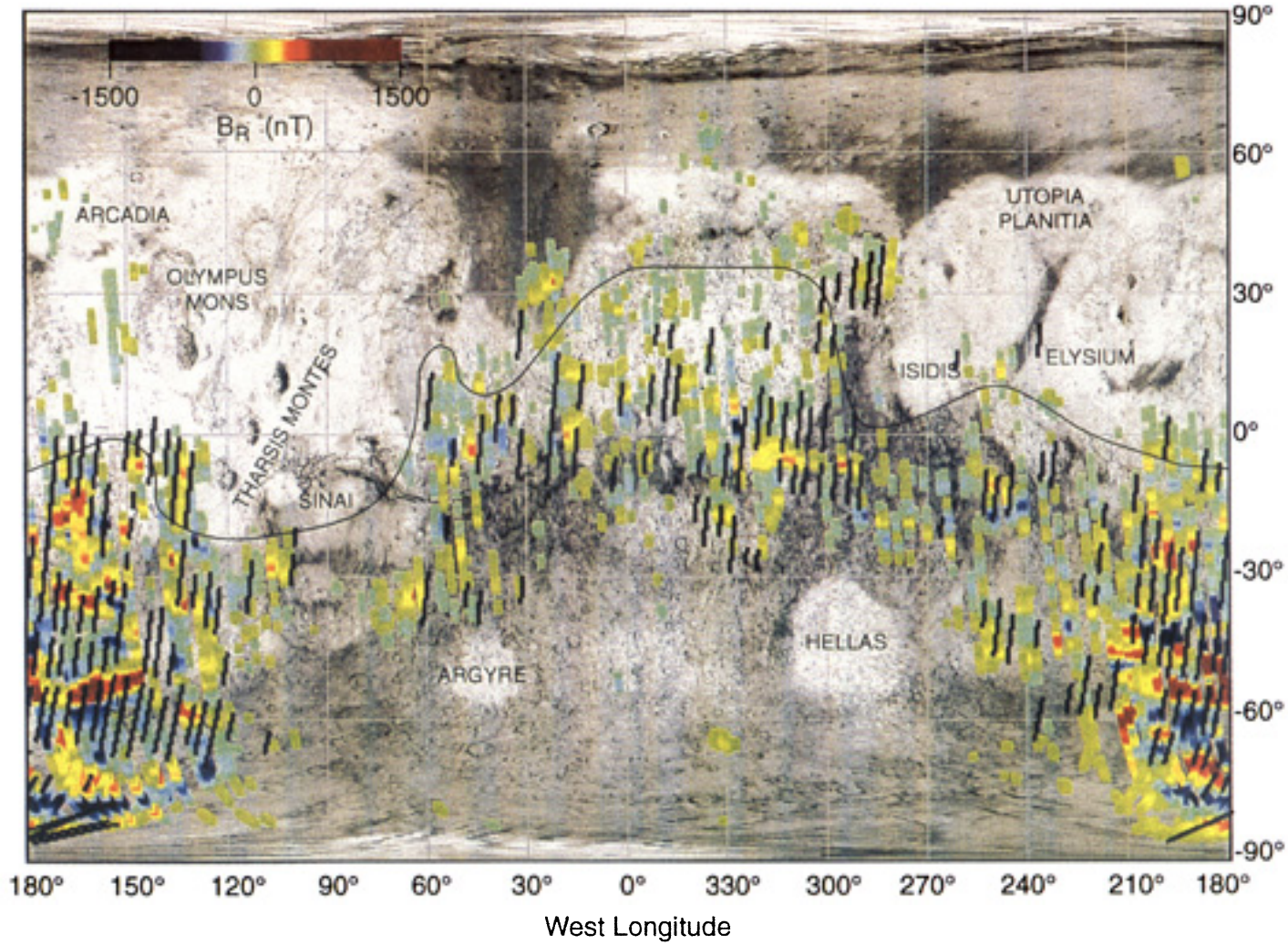

Plate 1. Map of the radial magnetic field component measured below 200-km altitude during aerobraking [*Acuña et al.*, 1999]. The crustal dichotomy boundary is indicated by the thin solid curve. Each thick black line marks an orbit segment during which the spacecraft was inside a plasma void. Data from 48 consecutive orbits (June 24–30, 1999) were used to produce this image. Plasma voids are closely associated with crustal magnetic sources. Over the most strongly magnetized region (120°–210°W) narrow gaps between the voids follow linear trends that are aligned with the magnetic sources. These gaps define the locus of electron flux spikes.

relatively weak magnetic anomalies in the northern hemisphere.

Intense crustal magnetic fields in the southern hemisphere are strong enough to form localized "magnetocylinders" that extend well above the 400-km spacecraft altitude. On the night hemisphere these magnetocylinders are marked by a series of plasma voids separated by electron flux spikes where the crustal field is radially oriented. The electrons on the radial field lines originate from the solar wind, indicating that these field lines were at one time connected to the solar wind. When these magnetocylinders rotate into sunlight, they trap newly created ionospheric plasma.

MGS Electron Reflectometer measurements at the 400-km mapping altitude provide an excellent tool for studying the extent and variability of Mars' ionosphere. During aerobraking the response of the ionosphere to crustal magnetic fields and solar EUV was likely obscured by extreme variability of the ionopause altitude, owing in part to the solar wind–ionosphere interaction. Between February 1999 and September 2000 the ER recorded more than 2.3 million electron energy spectra, which are uniformly distributed in longitude and latitude and cover a wide range of solar EUV fluxes. These data were obtained close to the median ionopause altitude that was observed at high solar zenith angles in the northern hemisphere during the science phasing period. Thus the spacecraft should make numerous ionopause crossings as the boundary moves up and down. The occurrence of ionospheric plasma at the mapping altitude could depend on several factors, including solar wind parameters, EUV flux, crustal magnetic field strength, and solar zenith angle. The large volume of mapping data should permit a statistical analysis of the ionospheric morphology and variability along the mapping orbit. Preliminary surveys of ionospheric plasma at mapping altitudes suggest that weak crustal fields are detectable by small but statistically significant increases in the occurrence rate of ionospheric plasma at the mapping orbit.

References

Acuña, M. H., et al., The Mars Observer Magnetic Fields Investigation, *J. Geophys. Res.*, *97*, 7799, 1992.

Acuña, M. H., et al., Magnetic field and plasma observations at Mars: Initial results of the Mars Global Surveyor mission, *Science*, *284*, 790, 1999.

Acuña, M. H., et al., Magnetic field of Mars: Summary of results from the aerobraking and mapping orbits, *J. Geophys. Res.*, this issue, 2001.

Brace, L. H., R. F. Theis, W. R. Hoegy, J. H. Wolfe, J. D. Mihalov, C. T. Russell, R. C. Elphic, and A. F. Nagy, The dynamic behavior of the Venus ionosphere in response to solar wind interactions, *J. Geophys. Res.*, *85*, 7663, 1980.

Brace, L. H., W. T. Kasprzak, H. A. Taylor, R. F. Theis, C. T. Russell, A. Barnes, J. D. Mihalov, and D. M. Hunten, The ionotail of Venus—Its configuration and evidence for ion escape, *J. Geophys. Res.*, *92*, 15, 1987.

Cloutier, P. A., et al., Venus-like interaction of the solar wind with Mars, *Geophys. Res. Lett.*, *26*, 2685, 1999.

Connerney, J. E. P., M. H. Acuña, P. Wasilewski, N. F. Ness, H. Rème, C. Mazelle, D. Vignes, R. P. Lin, D. Mitchell, and P. Cloutier, Magnetic lineations in the ancient crust of Mars, *Science*, *284*, 794, 1999.

Crider, D. H., et al., Evidence for electron impact ionization in the magnetic pileup boundary of Mars, *Geophys. Res. Lett.*, *27*, 45, 2000.

Elphic, R. C., and A. I. Ershkovich, On the stability of the ionopause of Venus, *J. Geophys. Res.*, *89*, 997, 1984.

Fox, J. L., and A. Dalgarno, Ionization, luminosity, and heating of the upper atmosphere of Mars, *J. Geophys. Res.*, *84*, 7315, 1979.

Knudsen, W. C., Solar cycle changes in the morphology of the Venus ionosphere, *J. Geophys. Res.*, *93*, 8756, 1988.

Mantas, G. P., and W. B. Hanson, Photoelectron fluxes in the Martian ionosphere, *J. Geophys. Res.*, *84*, 369, 1979.

Mitchell, D. L., R. P. Lin, H. Rème, D. H. Crider, P. A. Cloutier, J. E. P. Connerney, M. H. Acuña, and N. F. Ness, Oxygen Auger electrons observed in Mars' ionosphere, *Geophy. Res. Lett.*, *27*, 1871, 2000.

Ness, N. F., et al., MGS magnetic fields and electron reflectometer investigation: Discovery of paleomagnetic fields due to crustal remanence, *Adv. Space Res.*, *23*(11), 1879, 1999.

Øieroset, M., D. L. Mitchell, T.-D. Phan, R. P. Lin, and M. H. Acuña, Hot diamagnetic cavities upstream of the Martian bow shock, *Geophys. Res. Lett.*, *28*, 887, 2001.

Spenner, K., W. C. Knudsen, K. L. Miller, V. Novak, C. T. Russell, and R. C. Elphic, Observation of the Venus mantle, the boundary region between solar wind and ionosphere, *J. Geophys. Res.*, *85*, 7655, 1980.

Tobiska, W. K., and F. E. Eparvier, EUV97: Improvements to EUV irradiance modeling in the soft x-rays and FUV, *Sol. Phys.*, *177*, 147, 1997.

Vignes, D., C. Mazelle, H. Reme, M. H. Acuña, J. E. P. Connerney, R. P. Lin, D. L. Mitchell, P. Cloutier, D. Crider, and N. F. Ness, The solar wind interaction with Mars: Location and shapes of the bow shock and the magnetic pile-up boundary from the observations of the MAG/ER experiment onboard Mars Global Surveyor, *Geophys. Res. Lett.*, *27*, 49, 2000.

Zhang, M. G. H., J. G. Luhmann, A. J. Kliore, and J. Kim, A post-Pioneer Venus reassessment of the Martian dayside ionosphere as observed by radio occultation methods, *J. Geophys. Res.*, *95*, 14,829, 1990.

R. P. Lin and D. L. Mitchell, Space Sciences Laboratory, University of California, Berkeley, CA 94720. (mitchell@ssl.berkeley.edu.)

C. Mazelle and H. Rème, Centre d'Etude Spatiale des Rayonnements, 31028 Toulouse Cedex 4, France.

P. A. Cloutier, Department of Physics and Astronomy, Rice University, Houston, TX 77005.

M. H. Acuña and J. E. P. Connerney, NASA Goddard Space Flight Center, Greenbelt, MD 20771.

N. F. Ness, Bartol Research Institute, University of Delaware, Newark, DE 19716.

(Received November 30, 2000; revised June 15, 2001;
accepted July 30, 2001.)